

Research report

# The role of cell death during neocortical neurogenesis and synaptogenesis: implications from a computational model for the rat and mouse

Julia M. Gohlke, William C. Griffith, Elaine M. Faustman\*

*Center for Child Environmental Health Risks Research, Department of Environmental and Occupational Health Sciences, University of Washington, Seattle, WA 98105-6099, USA*

Accepted 29 March 2004  
Available online 11 June 2004

## Abstract

We are quantitatively evaluating the acquisition of neocortical neurons through key stages of development including neurogenesis, migration, and synaptogenesis. Here we expand upon a previous computational model describing neocortical neurogenesis in the rat and mouse [Dev. Neurosci. 24 (2002) 467], to include the period of synaptogenesis (P0–P14) when programmed cell death (PCD) is known to play a major role in shaping the neocortex. We also quantitatively evaluate differing hypotheses on the role of cell death during neurogenesis. This new model construct allows prediction of acquisition of adult neuronal number in the rat and mouse neocortex from the beginning of neurogenesis through synaptogenesis. The mathematical model output is validated by independently derived stereologically determined neuron number estimates in the adult rat and mouse. Simulations suggest cell death during synaptogenesis reduces the neocortical neuronal population by 20–30%, while cell death of progenitor cells and newly formed neurons during neurogenesis may reduce output by as much as 24%. However, higher death rates during neurogenesis as suggested by some research would deplete the progenitor population, not allowing for the vast expansion that is the hallmark of the mammalian neocortex. Furthermore, our simulations suggest the clearance time of dying neurons labeled by TUNEL or pyknosis is relatively short, between 1 and 4 h, corroborating experimental research. This novel mathematical model for adult neocortical neuronal acquisition allows for *in silico* analysis of normal and perturbed states of neocortical development as well as interspecies and evolutionary analyses of neocortical development.

© 2004 Published by Elsevier B.V.

*Theme:* Development and regeneration

*Topic:* Neuronal death

*Keywords:* Neocortex; Computational model; Neurogenesis; Synaptogenesis; Programmed cell death; Cell cycle kinetics

## 1. Introduction

The neocortex is thought to be the primary region for human thought, language, and behavior, and is the dominant structure of the mammalian brain [46]. During mammalian evolution, the neocortex has become an increasingly complex brain structure composed of at least six layers with 10 to 20 functional subdivisions, acting as representation maps of motor and sensory information. The basic function of the neocortex is the analysis and representation of the relation-

ship between the components of sensory and motor patterns, which in turn support functions such as perception, motor programming, memory, language processing, and reasoning [30]. The latter functions in particular have become increasingly refined during primate evolution and are thought to be the hallmark of human intelligence. Understanding the cellular mechanisms of neocortical development is necessary in order for us to understand the evolution of the structure and how perturbations during development may cause long-term neocortical related deficits.

A systems level approach, incorporating molecular, cellular, organ, and behavioral analyses, in neurodevelopmental research will greatly enhance our understanding of mechanisms of normal neurodevelopmental processes and perturbations that may lead to neurodevelopmental disorders [39]. Under this premise, we have built a general mathe-

\* Corresponding author. Department of Environmental Health, Institute for Risk Analysis and Risk Communication, University of Washington, 4225 Roosevelt Way NE, Suite #100, Seattle, WA 98105-6099, USA. Tel.: +1-206-685-2269; fax: +1-206-685-4696.

*E-mail address:* [faustman@u.washington.edu](mailto:faustman@u.washington.edu) (E.M. Faustman).

mathematical model at the cellular level for normal neocortical development that simulates acquisition of adult neuronal cell number through neurogenesis [29]. To strengthen our current computational model for neocortical development, we extend the model to include programmed cell death during the period of neocortical synaptogenesis, postnatal day 0 to postnatal day 14 (P0–P14) in the rodent (roughly the 3rd trimester equivalent in humans).

Programmed cell death (PCD), or apoptosis, is an integral part of the development of the central nervous system and it has been estimated up to half of the original cell population is eliminated as a result of apoptosis [45,53,56]. Apoptosis of young neurons is thought to optimize synaptic connections by removing unnecessary neurons, often referred to as the nerve growth factor theory [26]. This theory postulates during the critical synaptogenesis period, competition of neurons for their targets determines the amount of neurotrophic factors received by the developing neurons. The messengers in this system are neurotrophic factors released from the postsynaptic target that regulate the release of cytochrome *c* and caspase activation [53]. The programmed cell death period has been characterized in the rat, cat, mouse, and hamster neocortex [56]. This process has also been reproduced in numerous primary in vitro culture systems through growth factor deprivation in young neurons [17,18].

Recent research has implicated cell death may play a larger role in the earlier proliferative stages of neurodevelopment than previously thought [15,40,45]. For example, mice deficient in key apoptotic regulators, Caspase 3 and Caspase 9, show severe overgrowth of the ventricular region by E10.5, suggesting cell death plays a major role even before neurogenesis in the mouse [41,42]. Furthermore, (all throughout the file) Blaschke et al. [3], using a novel protocol for an in situ end labeling technique (ISEL+) to detect dying cells, found that on average 50% of the proliferating cells during neurogenesis (E12–E18) are dying at any one time. Using *Casp3*<sup>-/-</sup> mice, only 18% of the ISEL+ staining was explained through the Caspase 3 pathway [58]. Although this research suggests cell death may play an important role well before the classical synaptogenesis period from which the neurotrophic theory evolved, others have shown cell death plays a relatively minor role during neurogenesis [7,33,75]. There is a critical need for quantitative analyses estimating how much early cell death affects final neocortical neuronal numbers [15]. Here we quantitatively analyze this data through simulations with varying cell death rates in our neurogenesis model.

## 2. Materials and methods

As in our neocortical neurogenesis model, our extended mathematical model of neocortical synaptogenesis was developed using a generalized, stochastic model framework for developmental processes in which a cellular population

of relatively immature, undifferentiated cells going through periods of proliferation, differentiation, and apoptosis to form the final cell population, tissue, or organ of interest [44]. Here we develop several new applications of our generalized model. We have developed a murine neocortical synaptogenesis model and a rat neocortical synaptogenesis model that have been linked to our previously developed neurogenesis models. Therefore, the founder cell population of neurons in the neocortex is tracked through neurogenesis and synaptogenesis simulating the acquisition of final adult neocortical neuronal cell number.

Our extended model framework including programmed cell death (PCD) during the synaptogenesis period is illustrated in Fig. 1. The model construct has been described in detail previously [29]. The key model parameters include cell cycle rates ( $\lambda$ ), differentiation rates ( $\nu$ ), and cell death rates ( $\mu$ ) within a critical time period specific to the cell population, organ, or tissue of interest. Time-dependent normal mouse and rat neocortical neuronal death rates derived from analyses looking at neuronal cell death in various regions of the developing neocortex during synaptogenesis and neurogenesis in the mouse and rat are used as model inputs [26,66,75,76]. To evaluate the robustness of our model, we compare our model results with independent stereological estimates of adult neocortical cell number in the rat and mouse [5,8,21,50,51,68].

For three key parameters in our model construction, experimental studies suggest differing values. We have performed sensitivity analyses on variability of these key parameters, including the growth fraction (GF) during neurogenesis, the founder cell population at the start of neurogenesis ( $X_0$ ), and the clearance time of neurons undergoing cell death during neurogenesis and synaptogenesis. These simulations quantitatively show the differences in neuronal output predicted by our model based on experimentally derived differences in parameter estimations.

### 2.1. Model of neocortical neurogenesis

Our model for the process of neocortical neurogenesis has been previously described [29]. Briefly, experimental data describing normal murine and rat neocortical neurogenesis were used to determine parameter values for our model of murine and rat neocortical neurogenesis under normal development [48,70,72,73]. In our model, progenitor cells making up the pseudostratified ventricular epithelium (PVE) located in the developing rostral neural tube are referred to as “X cells”, and postmitotic young neurons leaving the PVE to migrate and subsequently populate the cortical plate are labeled “Y cells” (Fig. 1A,B). The X cells have a time-dependent division and differentiation rate, while the Y cell division rate is set to zero. The X cells divide producing a large progenitor proliferative (*P*) population. The X cell population gradually adds more cells to the Y cell population, or Quiescent (*Q*) population, which are young, postmitotic neurons beginning migration to the cortical plate (CP).

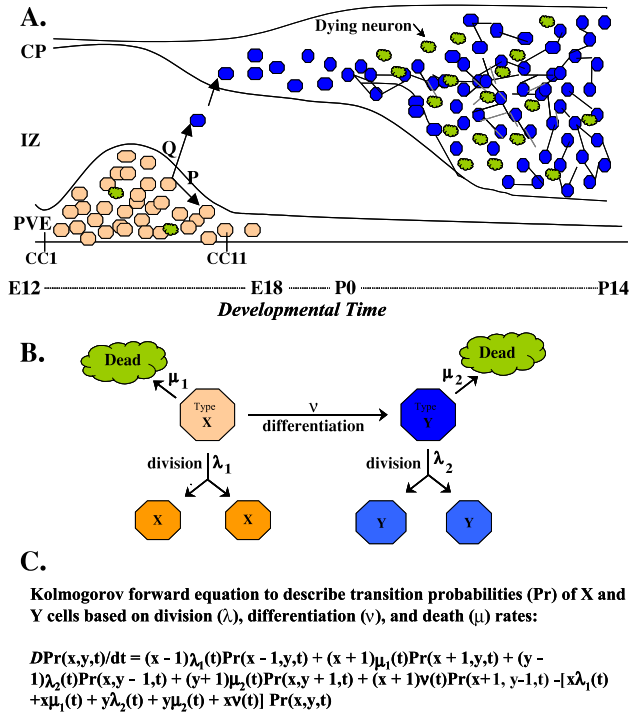


Fig. 1. Model framework for neocortical neuronal proliferation, differentiation, and cell death. (A) During neurogenesis (E11–E16 in mouse and E13–E19 in rat) progenitor cells are generated in the pseudostratified ventricular epithelium (PVE) through 11 cell cycles in the mouse (CC1–CC11). During G1 newly generated cells either stay in the proliferative population (P fraction) or become postmitotic (Q fraction) and begin migration through the intermediate zone (IZ) to the cortical plate (CP). Minimal cell death is thought to occur during this period. Differentiation along with more ubiquitous apoptosis of the new neuronal population takes place postnatally (P0–P14) in the mouse and rat neocortex. (B) Basic model framework from Leroux [44], which is color coded to illustrate model for neocortical neurogenesis where Type X cells represent neuronal progenitor cells in the PVE and Type Y cells represent postmitotic neurons leaving the PVE, emphasizing that the differentiation rate is dependent upon the division rate. In our model,  $Q = Y(t)/(X(t) + Y(t))$ , and  $P = GF(1 - Q)$ , where GF is the growth fraction or fraction of cells cycling. (C) The central differential equation of the model relating the probability of division ( $\lambda$ ), differentiation ( $v$ ), or death ( $\mu$ ) in the X or Y cell through time ( $t$ ). This equation is used to derive estimates of the number of X and Y cells present at time ( $t$ ) through a solution matrix (see Ref. [29]).

### 2.2. Model for programmed cell death during synaptogenesis

The period of programmed cell death for the rodent neocortex occurs between postnatal days 1 and 14 (P1–P14), with a peak between P4 and P7 and has been quantified by stereological examination of stained brain sections. Four studies have been identified that quantitatively analyze the temporal profile of PCD during normal synaptogenesis in the mouse and rat neocortex [25,66,75,76] (Fig. 2). Verney et al. [76], using TdT mediated dUTP nick end-labeling (TUNEL), which tags nuclear DNA fragments, reports TUNEL+/mm<sup>2</sup> on P0, P4, P6, P8, P10 and P14 in the parietal cortex (Fields 1, 3 and 40) of the

mouse. A TUNEL Labeling Index, or percent of total cells labeled, is reported for P0, P4, P8, and P14. A peak in TUNEL+ cells occurs at P4. Ferrer et al. [26] identifies average pyknotic cells/1000 live cells (condensed chromatin, nuclear fragmentation, and a pale cytoplasm) on postnatal days 2, 5, 7, 10, 15, and 21 in the primary visual, somatosensory and frontal cortex of the rat. A peak is reached at P7 in this analysis. Also using TUNEL staining to quantitate PCD over the synaptogenesis period on P1, P5, P8 and P14 in the somatosensory cortex of the rat, Spreafico et al. [66] shows the highest percent staining, with a peak at P5. Data from Thomaidou et al. [75] looking at average TUNEL staining on P0, P7, and P14 throughout the developing rat neocortex, suggests a peak at P0. Others have also suggested an earlier peak in postnatal programmed cell death in the rat [71]. It has been suggested that both TUNEL labeling and identification of pyknotic nuclei may lead to false positive results in some instances, however both methods are considered the most appropriate for quantitating cell death in slices of tissue where intact morphological boundaries are important [57].

Very few studies have attempted to quantitate the clearance time, which is the amount of time between staining of the cell destined for programmed cell death and the actual disappearance of that cell. For our analysis, this quantitative information is critical in defining a cell death rate ( $\mu$ ) for our model. Thomaidou et al. [75] has published the only in vivo study estimating the clearance time of TUNEL+ cells in the developing neocortex of the rat. This study uses a double labeling procedure to elucidate

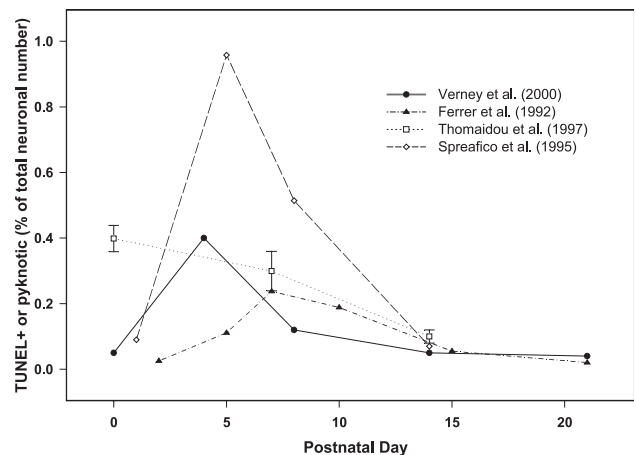


Fig. 2. Comparison of quantitative, time-dependent analyses of cell death during the postnatal synaptogenesis period in the mouse and rat neocortex. Verney et al. [76]: TUNEL+ in Fields 1, 3 and 40 (layers I–VI) of parietal cortex of mouse ( $n=4$  per time point). Ferrer et al. [26]: Pyknotic nuclei in neocortex defined as area between callosal and rhinal fissures (layers I–VIb) in rat ( $n=2-3$  per time point). Thomaidou et al. [75]: TUNEL+ in total developing neocortex of rat ( $n=6$  on P0;  $n=2$  on P7, P14). Error bars represent 95% CI. Spreafico et al. [66]: TUNEL+ in somatosensory cortex (layers II–VIa) of rat. The minimum sample size included one animal with quantification of three, nonserial sections for each time point within the somatosensory cortex [66].

the clearance time of TUNEL+ cells in the proliferative population of the subventricular zone in newborn rats (P0). The procedure labels a cohort of cells, proceeding in synchrony through the cell cycle labeled only with BrdU, as [<sup>3</sup>H]thymidine is sequentially injected after the initial BrdU injection to double label other proliferating cells. They found cells were labeled with TUNEL in G1, and it took approximately 2.5 h for them to disappear. They corroborated TUNEL+ staining with analysis of pyknotic cells. The calculation of the clearance time assumes that the length of mitosis and the length of apoptosis remain approximately constant during the analysis.

For our model we determined a time-dependent postnatal cell death rate based on the Thomaidou et al. [75] clearance time of 2.5 h and the four studies described above quantitatively analyzing TUNEL+ and/or pyknotic neurons throughout synaptogenesis in the rodent. This clearance time was also used in our neurogenesis model, the model of Haydar et al. [34] to determine a cell death rate during neurogenesis, and Verney et al. [76] to determine proportionate cell loss in the postnatal mouse [29]. When using this clearance time we are assuming the clearance time of TUNEL+ neurons seen postnatally during synaptogenesis is similar to the clearance time in proliferating cells of the subventricular region at PND0.

We start simulation at P0 and go through P14, encompassing the peak synaptogenesis period in the rat and mouse model. We assumed a constant death rate on each day of synaptogenesis. Each day has a Y cell death rate ( $\mu_2$ ) based on regressions of the four experimental studies analyzing % TUNEL+ or % pyknotic (Fig. 2). The death rate ( $\mu_2$ ) is calculated by the following equation:

$$\mu_2(t) = [\ln(1 - (\%TUNEL(+)) / 100) \times 24 \text{ h}] / Cl.$$

where Cl is 2.5 h based on the experimentally determined clearance time of TUNEL+ cells in the subventricular region of the neocortex at PND0 [75]. Verney et al. [76] also calculates proportionate cell loss in the developing mouse neocortex using the clearance time of Thomaidou et al. [75]. The X and Y cell division rates ( $\lambda$ ) and the transformation rate ( $\nu$ ) are set to zero in our synaptogenesis models, as the Y cell population represents postmitotic,

growth factor-dependent young neurons forming synapses in the cortical plate.

### 2.3. Cell death during neurogenesis

To analyze the cell death rate during neurogenesis ( $\mu_1$ ), we change the % TUNEL+ up to 50%, reflecting the cell death labeling using ISEL+ staining (also looking at fragmented DNA) of Blaschke et al. [3] (see Table 2). We also evaluate data suggesting only 18% of this cell death can be accounted for by the Caspase 3 pathway [58]. We simulate several other TUNEL and pyknosis labeling analyses of cell death during neurogenesis, as these are common procedures used to quantitate cell death [36,37,62,75]. We use the same equation as in the synaptogenesis model described above to calculate the cell death rate. We also vary the clearance time up to 48 h, reflecting the possibility of the ISEL+ labeling procedure showing increased sensitivity, labeling cells that are destined to die as much as 48 h in advance.

### 2.4. Analysis of the growth fraction (GF), founder cell number, and clearance time

We evaluate inter experimental variability in key model parameters (Table 1). Our analysis of the growth fraction (GF), or percent of progenitor (X) cells actively cycling, in the neurogenesis model involved changing the previously used constant GF of 93% [29], to 80%, 97%, and 100% based on several experimental measures of this parameter [6,47–49,70]. In another simulation we varied the GF through time according to Miyama et al. [49] starting with a GF of 100% on E11 (E13 in rat) and decreasing it approximately linearly through time to 83% on E16 (E19 in rat). Founder cell number ( $X_0$ ) was also varied in the rat model to reflect the potential inappropriate use of a mouse founder cell population estimate in the rat model, as the rat embryo is overall larger, thereby most likely having more cells at the beginning of neurogenesis. The founder cell population was increased by 20% ( $6 \times 10^5$ ) and 40% ( $7 \times 10^5$ ), respectively, from the experimentally derived mouse founder cell population of  $5 \times 10^5$  [34]. In our analysis of the clearance time during synaptogenesis, we change the clearance time to 1 or 4 h, based on several in vitro analyses [2,31,35,59].

Table 1  
Variability analyses of key parameters in model

Parameter	Definition	Range evaluated	Species	References
Growth fraction (GF)	$GF = P(t)/X(t)^a$	80–100%	Mouse and rat	[6,34,47–49,69,70]
Clearance time (Cl)	See equation for death rate ( $\mu_2$ ) in text	1–4 h	Mouse and rat	[2,17,35,59,75]
Founder cell population ( $X_0$ )	# of X cells present at beginning of neurogenesis	$5-7 \times 10^5$ cells	Rat	[34]

<sup>a</sup> Where  $P(t)$  is the number of cells actively cycling time  $t$ .

### 3. Results

#### 3.1. Model for programmed cell death during synaptogenesis

The time-dependent cell death rates calculated using the four studies described above and illustrated in Fig. 2 were used to extend our neurogenesis model to include PCD during the synaptogenesis period, predicting adult neocortical neuronal number and comparing these values with independent stereologically determined neuronal counts in the adult neocortex of the mouse and rat (Fig. 3). The use of the Verney et al. [76] and Thomaidou et al. [75] dataset predicts a 21% and 30% ( $1.6$  and  $1.4 \times 10^7$  total neurons in the rat) neuronal loss during the synaptogenesis period in the rat and mouse. When using the Ferrer et al. [26] data set our model predicts the least neuronal loss at 16% ( $1.7 \times 10^7$  in the rat), while using the Spreafico et al. [66] dataset predicts the greatest loss at 48% ( $1.0 \times 10^7$  in the rat) of neocortical neurons.

For independent comparisons, stereologically determined data indicate total adult murine neocortical neuronal number between  $1.0$  and  $1.2 \times 10^7$  [5,8]. Previous stereological studies using a different approach estimating density of neurons per  $1 \text{ mm}^2$  of cortical surface and total area agree with the design-based stereological estimates of neuron number [32,63,65]. For the adult rat neocortex, stereologically determined mean estimates between  $1.5$  and  $2.1 \times 10^7$  neurons have been published [21,50,51,67,68].

#### 3.2. Cell death during neurogenesis

To determine our cellular death rate ( $\mu$ ) in our original neurogenesis model, we applied the results of Haydar et al. [34] in which cell death was measured using TUNEL

staining on E15–E18 in the mouse neocortex along with the assumption of a clearance time of 2.5 h based on Thomaidou et al. [75], [29]. We treat the X and Y cell death rate as identical during neurogenesis based on Thomaidou et al. [75], which showed that during the neurogenesis period in both the ventricular zone and the cortical plate the % pyknotic and TUNEL+ cells is very low and approximately equal [75].

We have varied our cell death rate in our neurogenesis model to reflect the range in experimental data using TUNEL or pyknosis, two common measures of cell death, in the amount of cell death occurring during this critical stage of development (Table 2). We have compared simulations of neurogenesis with no cell death to simulations with rates of cell death reflective of the data presented in Haydar et al. [34], Thomaidou et al. [75], Reznikov and Van der Kooy [62], and Hoshino et al. [36,37] looking at pyknotic cells or using TUNEL staining. Simulations with these experimental studies suggest between 1% and 24% of progenitor cells and young postmitotic neurons may die during the neurogenesis period. We also model the data of Blaschke et al. [3] using the ISEL+ protocol for labeling dying cells. In simulations run where the clearance time is kept at 2.5 h, the model predicts the proliferative and postmitotic population will be completely depleted by day 2 of neurogenesis if the Blaschke et al. [3] data is used. Based on the authors' suggestion that ISEL+ is especially sensitive and may identify dying cells long before other labeling techniques such as TUNEL, we increased the clearance time up to 48 h in our simulations. With a clearance time of 48 h, our model predicts only  $0.28 \times 10^7$  neurons generated during neurogenesis, approximately 23% to 28% of independent stereological estimates predicting between 1 and  $1.2 \times 10^7$  neurons in the adult mouse cortex (without taking into account postnatal cell

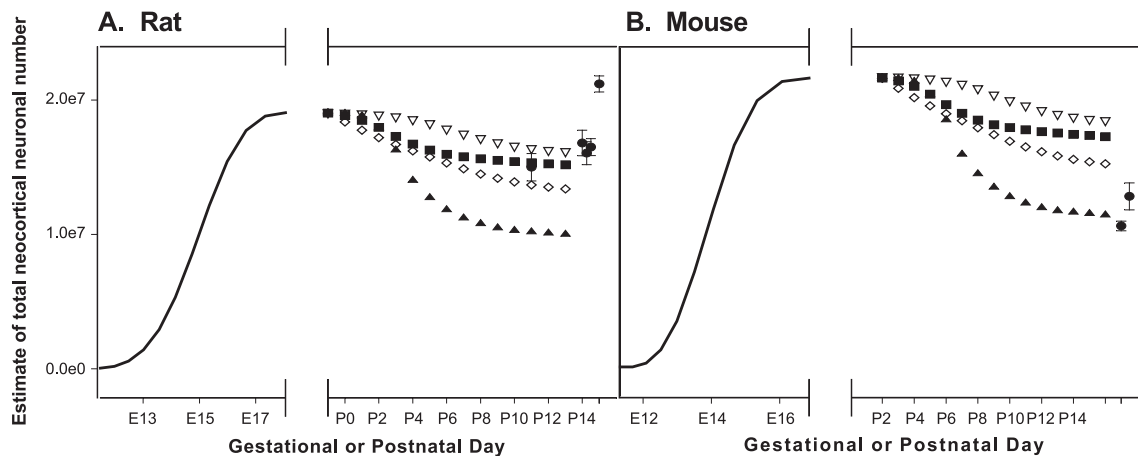


Fig. 3. Rat and mouse neocortical neuronal output predictions through neurogenesis and synaptogenesis. This figure shows a plot of our model predictions for the normal rat (A) and mouse (B) neuronal output (total Y cells). For comparison we plotted stereological estimates ( $\pm$  S.E.M.) of total neurons in the neocortex of the adult rat and mouse ( $\bullet$ ) etc. [5,8,21,50,51,65,68]. Four studies looking at time-dependent cellular death (pyknosis or TUNEL+ percentages) during postnatal development in the rat and mouse were applied to the model and compared to the independent, stereologically determined neuronal number data [26] ( $\blacktriangledown$ ); Verney et al. [76] ( $\blacksquare$ ); Thomaidou et al. [75] ( $\diamond$ ); and Spreafico et al. [66] ( $\blacktriangle$ ). The clearance time is assumed to be 2.5 h in all cases [75].

Table 2  
Simulations applying different measures of cell death during neurogenesis

Reference	Embryonic day/s <sup>a</sup>	Method used	Percent cells labeled	Clearance time (h)	No. of neurons generated (in millions)	Percent neurons generated <sup>b</sup>
–	–	–	0	–	21.5	100
Haydar et al. [34]	E14–E17	TUNEL	0.014	2.5	21.4	99
Reznikov and Van der Kooy [62]	E13–E14	Pyknosis	0.13	2.5	20.2	94
Hoshino et al. [36]	E10, E13, E15	Pyknosis	0.4, 0.2, 0.06	2.5	19.4	90
Hoshino et al. [37]	E13	Pyknosis	0.2	2.5	19.1	88
Thomaidou et al. [75]	E13	TUNEL	0.5	2.5	16.4	76
Blaschke et al. [3]	E12–E18	ISEL+	50	2.5	0	0
				24	0.37	2
				48	2.8	13
Pompeiano et al. [58] <sup>c</sup>	E12	ISEL+	18- <i>Casp3</i> dependent	2.5	0	0
				24	6.7	31
				48	11.8	55

<sup>a</sup> Experimental data indicating % of cells labeled during neurogenesis in the rat [62,75] or mouse [3,34,36,37,58]. When multiple days are analyzed, an average of the % cells labeled is utilized, except for data from Hoshino and Kameyama [36] in which a time-dependent rate was used.

<sup>b</sup> The reduced output of the neurogenesis model as a percentage of the cells generated when no death during neurogenesis is assumed (first row).

<sup>c</sup> This research assessed the percent of cells labeled with ISEL+ in the wild type mouse versus the percent ISEL+ labeled cells in the *Casp3* –/– mouse.

death during synaptogenesis). These simulations suggest cell death may not be as common during neurogenesis as the Blaschke et al. [3] data proposes. We also modeled data from studies in *Casp3* –/– mice suggesting the Caspase 3 accounts for only 18% of the ISEL+ staining in the normal mouse [58]. Simulations based on Caspase 3-dependent ISEL+ labeling again predict a total depletion of cells when a clearance time of 2.5 h is used. When a clearance time of 48 h is used  $1.18 \times 10^7$  neurons are generated. However, this number would be expected to decrease by 20% during the synaptogenesis period, again under predicting the amount of neurons in the adult mouse neocortex.

### 3.3. Analysis of the growth fraction, founder cell number, and clearance time

The growth fraction (GF), or percentage of progenitor cells actively cycling, is an important experimental parameter in our neurogenesis model [29]. Here we perform an analysis based on inter-study variation in GF estimations to establish the importance of this parameter on the final output of neuronal number (Fig. 4A,B). Experimental estimates of this parameter in the proliferative zone (ventricular zone or pseudostratified ventricular epithelium) during neocortical neurogenesis (E11–E16 in mouse and E13–E19 in the rat)

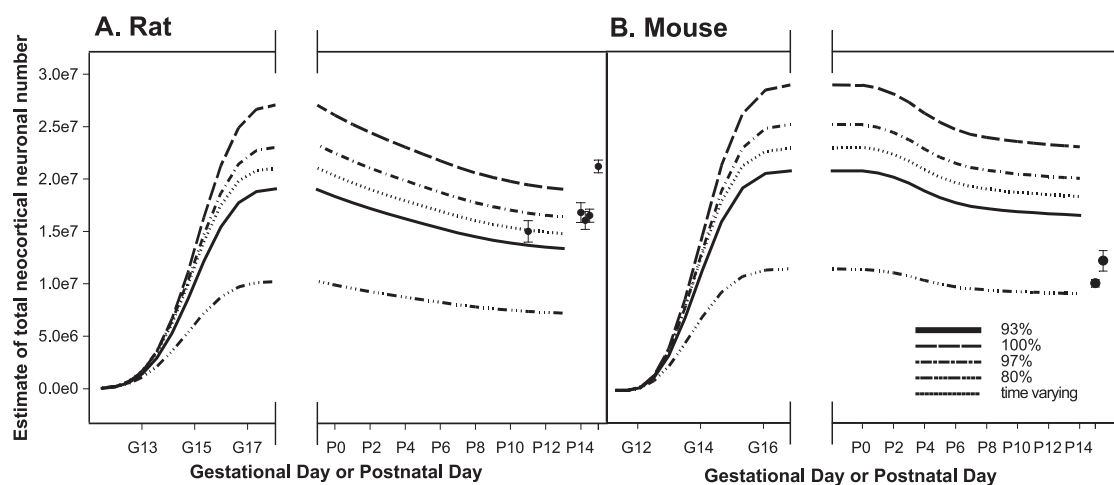


Fig. 4. Analysis of experimental variation for the growth fraction (GF) parameter in our neocortical neurogenesis model. Analyses was performed to examine various growth fraction (GF) estimates: 80% in mouse [6] and rat [48], 93% in mouse [34] and rat [47], 97% in mouse [69] or 100% in mouse [70] of cells actively cycling or a time-dependent GF with 100% at beginning of neurogenesis and falling to 80% at end of neurogenesis in mouse [49]. (A) Analysis of the growth fraction (GF) parameter in rat model using the Thomaidou et al. [75] dataset for synaptogenesis model for rat (B). Analysis of the growth fraction (GF) parameter in mouse model using the Verney et al. [76] dataset for synaptogenesis model. Stereological estimates ( $\pm$  S.E.M.) of total neuronal number are plotted for comparison (●) (see Fig. 3 caption for references).

range from 80% to 100% [6,47–49,70]. Furthermore, time-dependent data from Miyama et al. [49] suggests the GF decreases from 100% on E11 to 83% on E15 in the mouse. Here we compare four fixed estimates of GF including 100%, 97%, 93%, and 80% throughout neurogenesis. We also simulate GF as a time-dependent parameter as the data of Miyama et al. [49] suggests.

Varying the growth fraction between 80% and 100% in our model significantly alters our predictions of final neuronal number. The final neuronal output is reduced by 45% when GF is reduced from our original estimation of 93% to 80%. Increasing the GF to 100% increases the final output by 42%. When a time-dependent GF is used to reflect the findings of Miyama et al. [49], the final neuronal output is increased by 12% over our original estimations using a constant GF of 93%.

In the current rat model we are using the experimentally derived mouse founder cell population ( $X_0$ ) from Haydar et al. [34]. However, based on overall differences in body size, this may not be optimal. We performed a sensitivity analysis of this parameter in which the founder cell population ( $X_0$ ) is increased in the rat model by 20% and 40%, respectively. This analysis gives a large increase in the final output (Fig. 5). The final neuronal number prediction is  $1.6 \times 10^7$  and  $1.9 \times 10^7$ , respectively, compared with  $1.3 \times 10^7$  when the original mouse founder cell population is used in the rat model. As is apparent in Figs. 4 and 5, increasing the amount of young neurons produced in our rat neurogenesis model, either by increasing the GF or by increasing the founder cell population, produces simulations that more closely predict the independent stereological data.

Our analysis on the clearance time used to determine the death rate ( $\mu_2$ ) in our synaptogenesis model was based on comparisons of various in vivo and in vitro estimates. In vitro studies of apoptosis can inform our analysis as they allow us to investigate specific mechanistic hypotheses. Normal apoptosis during synaptogenesis is thought to occur because neurons are not receiving enough growth factor due to insufficient connections. In a recent review of in vitro systems, Deshmukh and Johnson [18] show Fas-mediated PCD can be as fast as 4–6 h, but trophic factor deprivation induced PCD lasts between 24 and 48 h [19]. For cultures of NGF-dependent neonatal rat sympathetic neurons deprived of NGF, no morphological changes occurred during the first 12 h [17]. When comparing graphs of the time course of DNA fragmentation versus loss of viability in this culture system, an average clearance time of approximately 4 h is evident [17].

Alternatively, in the glial-derived oligodendrocytes of the developing rat optic nerve, a clearance time estimation of 1 h was made based on number of total cells, % pyknotic cells at any one time and the % cells undergoing DNA synthesis [2,59]. A similar clearance time has been estimated through direct observation of the normal development of *C. elegans* [22]. A clearance time estimate of only 45 min for pyknotic cells in the developing rat retina was made by comparing the proportion of pyknotic cells and change in total cell numbers through time [78]. Using a similar methodology, clearance time was approximated at 3 h in developing retinal ganglion cells after tectal lesions [31]. Alternatively, injection of kainic acid into the eye producing cell death similar to trophic factor deprivation, indicated a clearance time of

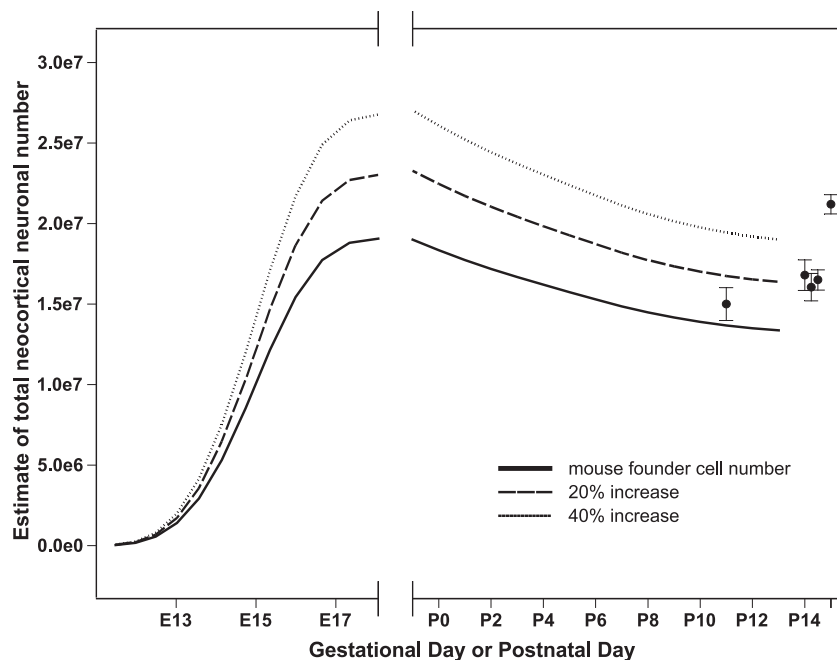


Fig. 5. Analysis of the founder cell population estimate in the rat neurogenesis model. The founder cell number ( $x_0$ ) was increased by 20 (to  $6 \times 10^5$ ) and 40% (to  $7 \times 10^5$ ) from the experimental estimate in the mouse of  $5 \times 10^5$  [34], to reflect the larger size of the rat brain at the beginning of neurogenesis.

approximately 4 h [35]. Other estimates of clearance time for dying neurons include 1.4 h for fetal mouse motor neurons and 3.2 h for dying neurons in the tadpole ventral horn [31].

These *in vivo* and *in vitro* analyses of various cell types are consistent with Thomaidou et al.'s [75] *in vivo* study of TUNEL+ cells disappearing after approximately 2.5 h, however it is important to quantitate the change in our model predictions based on the variability of estimates for the clearance time. Therefore, we ran simulations in our rat and mouse models in which the clearance time was varied between 1 and 4 h, encompassing the highest and lowest estimates from the experimental studies examined above.

In the rat analysis we chose the Thomaidou et al. [75] dataset for % of cells dying at each time point for our baseline model, as this dataset was the most complete dataset analyzing neuronal death in the whole neocortex through the synaptogenesis period (see Figs. 2 and 3A). Our analysis shows considerable changes to the output predictions based on this changing clearance time (Fig. 6A). When the clearance time is set to 1 h approximately 36% more cells are predicted to die in the mouse compared with the clearance time set at 2.5 h. Therefore, the total reduction of neurons due to PCD during synaptogenesis is predicted at 55% when the clearance time is 1 h versus only 32% when the clearance time is 2.5 h. However, when the clearance time is 4 h only 19% of the neurons are predicted to die over the synaptogenesis period in the rat.

For our mouse baseline model we chose the Verney et al. [76] dataset for the % cells dying, as this was one of the most thorough studies looking at neuronal death through the synaptogenesis period in the mouse parietal cortex (see Figs. 2 and 3B). When the clearance time is set to 1 h approximately 29% more cells are predicted to die in the mouse compared with the clearance time set at 2.5 h (Fig. 6B). The

total reduction of neurons due to PCD during synaptogenesis is predicted at 44% ( $1.2 \times 10^7$  neurons) versus only 21% ( $1.7 \times 10^7$  neurons) when the clearance time is 2.5 h. However, when the clearance time is 4 h only 13% ( $1.9 \times 10^7$  neurons) of the neurons are predicted to die over the synaptogenesis period in the mouse.

#### 4. Discussion

We have developed a computational model for rat and mouse neocortical development that includes neurogenesis and programmed cell death during synaptogenesis. To validate our models we compare our results to independently derived stereologically determined cell number data in the mouse and rat neocortex.

Our synaptogenesis model is robust when compared with independent estimates of percentages of neurons lost during this period. Independent data on neuronal number reduction in the neocortex due to PCD during synaptogenesis falls between 25% and 35% [4,26,75,76], although some have suggested as much as 50% neuronal loss in some regions [12]. Based on direct cell counts through the synaptogenesis period, Heumann and Leuba [79] suggest a 32% neuronal loss between P5 and P20 in the mouse cerebral cortex. Miller [80] analyzed the survival of [ $^3$ H]thymidine labeled cohorts through development into adulthood (injected on G15–G18 and analyzed on P60) and suggested a 20% neuronal loss in the mature rat somatosensory cortex. In the cat, direct cell counts suggest a cumulative neocortical neuronal loss of approximately 20% between birth and 6 months of age [24]. Verney et al. [76] estimated a 20% reduction in Field 1 of the parietal cortex based on the Thomaidou et al. [75] clearance time of 2.5 h. Our simu-

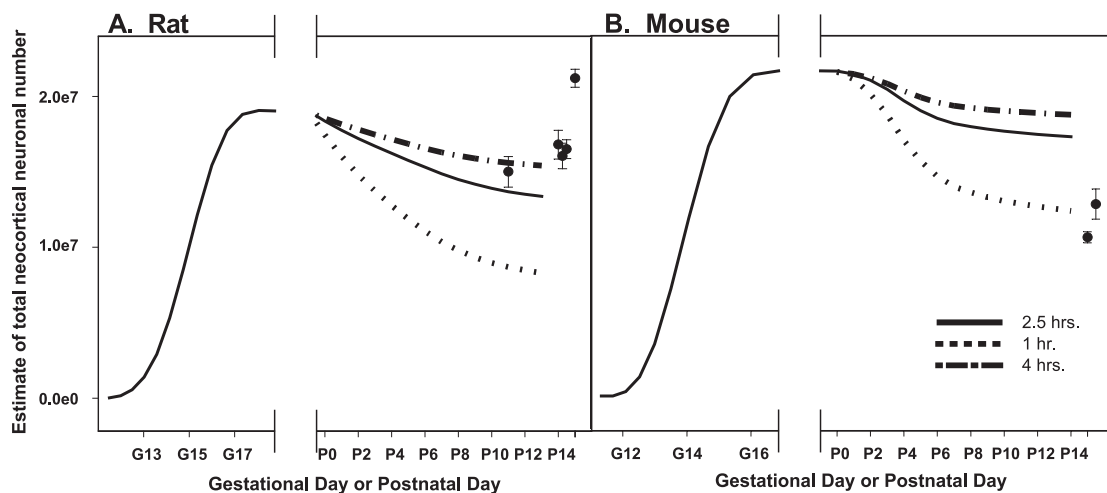


Fig. 6. Analysis of the impact of inter-experimental variability in clearance time estimates for TUNEL+ and pyknotic nuclei in neocortical synaptogenesis model. We varied estimations of death rates during the postnatal differentiation period based on differing estimations of clearance times in the rat model using the Thomaidou et al. [75] dataset for the rat model (A) and using the Verney et al. [76] dataset for the mouse model (B). Clearance times shown are 1 h [2,59], 2.5 h [75], and 4 h [17,35]. Stereological estimates ( $\pm$  S.E.M.) of total neuronal number are plotted for comparison ( $\bullet$ ) (see Fig. 3 caption for references).

lations using the Verney et al. [76] time-dependent TUNEL staining data suggest a similar neuronal loss (21%) over the synaptogenesis period in the neocortex of the mouse. Nunez et al. [81] estimated total neuronal loss in the visual cortex at 33% in male rats and 46% in female rats based on time-dependent percentages of pyknotic cells visible between P2 and P35 and fitting to stereological data estimating the adult sex differences in neuron number.

Analysis of inter-study variation for the growth fraction parameter in the neurogenesis model indicates predictions based on less than 100% of the progenitor population actively cycling are more robust when compared with stereological data in the adult mouse. This hypothesis is supported by numerous experimental data suggesting a GF between 80% and 93% during neurogenesis [6,34,47–49,69]. However, our mouse neurogenesis model, based on the experimental data of Takahashi et al. [70–72], predicts generation of more neurons than our rat model, which is based on the work of Miller and Kuhn [48]. There are some key differences in these data sets that may explain this discrepancy. Takahashi et al. [70,71] determines the cell cycle length on each day of the 6-day neurogenesis period in the mouse (E11–E16), while Miller and Kuhn [48] look at every other day in the rat (E13, E15, E17, E19). Also, unlike the  $P$  fraction in Takahashi et al. [72], which is explicitly derived from the PVE proliferative population, the GF determined by Miller and Kuhn [48] includes the subventricular region (SVZ) as well as the ventricular (VZ) proliferative populations. At late time points (E17 to E19), the discrepancy between the GF and  $P$  fractions may cause an overall increase in output in the rat model, as is suggested by the work of Takahashi et al. [70,71] in the mouse [71]. However, a recent report using retroviral labeling in conjunction with time-lapse microscopy of organotypic slice cultures, suggests cortical neurons do arise from the SVZ proliferative population between E17 and E19 in the rat [54], suggesting inclusion of this population in our rat model is justified. Furthermore, in both models, we use the starting cell number ( $X_0$ ) estimated from a stereological study in the mouse at E11 [33]. There may be important species differences in the pre-neurogenetic period when progenitor cell number is thought to increase exponentially [33]. Since the brain of the rat is significantly larger than the mouse brain at the beginning of neurogenesis, the founder cell population in the rat is most likely larger. A sensitivity analysis of this parameter in which the founder cell population ( $X_0$ ) is increased in the rat model by 20% and 40%, increased the final neuronal output by 23% and 46%, respectively. Therefore, increasing the founder cell population produces better predictions when compared to the independent stereological data in the rat model. This sensitivity analysis of the founder cell population is also relevant to the Caspase 3 and 9 knockout mice showing an increased progenitor population at the beginning of neurogenesis, possibly due to decreased apoptosis prior to neurogenesis [41,42].

In our rat model, sensitivity analysis of the clearance time of neurons undergoing PCD during synaptogenesis suggest a longer clearance time matches more closely with stereological data in the adult. With a clearance time of 4 h, 19% of the neurons are predicted to die over the synaptogenesis period, agreeing well with the direct cell count studies described above. In our mouse model, a shorter clearance time appears more robust when compared with adult stereological data. A well-designed in vivo study comparing pyknotic cells against reduction in cell number through time in the developing rat retina estimates a clearance time of only 45 min [78]. However, when the clearance time is set to 1 h in our model, total neuronal reduction after synaptogenesis is predicted at 44%, which is somewhat higher than direct cell count studies described above indicate. Most estimates of clearance time of pyknotic or TUNEL+ cells indicate that cells undergo degeneration and phagocytosis rapidly during normal neuronal death, as both of these markers are at the end stages of cell death [56]. However, it would be expected that variation in clearance times may occur at different developmental stages and following differing experimental manipulations (e.g. ethanol induced apoptosis). For example, massive cell death caused by exposure to a toxicant may overwhelm the macrophage clearance system, therefore temporarily lengthening the clearance time [35]. Also, species related differences in clearance times may be an important source of variation.

Knockout mice of key apoptotic regulators including Caspase 3 and Caspase 9 have shown apoptosis may play a significant role in establishing the founder cell population before neurogenesis, as these mutations cause severe overgrowth of the ventricular region by E10.5 [41,42]. However, the neurodevelopmental abnormalities associated with deletion of Caspase 3 have been shown to be strain-dependent [43]. When Caspase 3<sup>-/-</sup> mice were analyzed using ISEL+ on E12, 20% of cells were still labeled by ISEL+ relative to 50% in the controls suggesting either the Caspase 3 pathway is not the only pathway of cell death during neurogenesis or that the ISEL+ method is falsely labeling viable cells [58]. In fact, in a study of DNA damage induced cell death in neural precursor cells, cell death was not Caspase 3-dependent [20]. Therefore, apoptosis of progenitor cells before and during neurogenesis and apoptosis of postmitotic neurons during synaptogenesis may utilize different cell death pathways and serve distinct roles during neurodevelopment [33,40].

Our simulations suggest cell death may not play as large of a role during neurogenesis as the Blaschke et al. [3] data suggests, even when only Caspase 3-dependent ISEL+ labeling is modeled, as no neurons are generated when a clearance time of 2.5 h is used. However, there is the possibility that the clearance time of ISEL+ cells is longer because it is a more sensitive detection method. Our simulations suggest even with a clearance time of 48 h, which is the longest the complete cell death process has been estimated [17], the Blaschke based cell death rates still

vastly underestimate the amount of neurons produced. It has been suggested the ISEL+ method may be too sensitive, detecting cells with only transient DNA breaks [40]. Reports have suggested non-homologous recombination may be an important process during neurodevelopment as well as immunology in giving cells distinct identities [11,27,28,61]. This hypothesis is partly based on mice deficient in DNA ligase showing early neural cell death [64]. If transient DNA breaks are a common phenomenon in developing neurons, this may account for the results of Blaschke et al. [3]. Recently, *Dscam*, a gene required for correct axonal guidance in *Drosophila* neurons, has been shown to have over 38,000 variant splice forms, which are differentially expressed in neighboring neurons, leading to a distinct signatures of individual cells [52].

The Thomaidou et al. [75], Reznikov and Van der Kooy [62] and Hoshino et al. [36,37] datasets suggest a higher cell death rate during neurogenesis than the previously used Haydar et al. [34] dataset. Simulations with these experimental studies are compatible with the independent stereologically determined neuronal number data, suggesting between 6% and 24% cell loss during the neurogenesis period. In fact, if 16 million neurons are generated during neurogenesis as our model suggests using the Thomaidou dataset (Table 1) and approximately 20% are lost during synaptogenesis (Fig. 3), the final neuronal number would be consistent with the independent data at 13 million neurons in the adult mouse neocortex [5,8]. Elegant research modeling retrovirally marked lineages suggest less than 1% of neuronal progenitor cells per cell cycle are lost during the neurogenesis period in the mouse [7]. Based on the 11 cell cycle neurogenetic interval, this study agrees well with model predictions suggesting less than 10% total cell loss during neurogenesis (see Table 1). Studies in developing human brains show between 0.2% and 0.6% of cells labeled TUNEL+ during early and mid gestation [1,60], suggesting low cell death rates during human neocortical development consistent with the rodent studies showing similar percent labels between 0.1% and 0.4% [36,37,62,75] (Table 1).

Our current model of neocortical neuronal acquisition through the developmental processes of neurogenesis and synaptogenesis highlights the significance of these processes in shaping the adult neocortex. The power of computational models to integrate experimental data into hypotheses of mechanisms of developmental processes is being realized [10,13,16,55]. While recent computational models of development using genomic networks evaluate developmental changes at the molecular level, these models do not explicitly take into account the events of proliferation or death at the cellular level [14,74,77]. A recent report demonstrates the benefits of taking a systems level approach by combining a cellular level model of neurogenesis with p27 knock-out data to simulate p27 effects on the  $Q$  fraction during neurogenesis [9].

However, there have been limited applications of computational approaches for perturbations of neurodevelop-

mental processes in the context of risk evaluations [23,38]. The importance of the current model is its systematic and thorough analysis of differing experimental research on neocortical neuronal production and death. This endeavor highlights the importance of mathematical modeling in quantitatively comparing competing hypotheses of neocortical neuronal acquisition. Furthermore, the computational approach taken here sets bounds on key parameters such as the growth fraction, clearance time, and death rates during neurogenesis and synaptogenesis in the developing rodent neocortex. Through developing both a mouse and rat model, key interspecies differences in parameters can be evaluated. Most importantly, modeling biological processes using experimental data is a hypothesis generating exercise identifying important and specific experimental research needs to evaluate the key assumptions of our theories.

### Acknowledgements

This research was funded by the Center for Child Environmental Health Risks Research through EPA grant R826886, NIEHS grant 1P01ES09601, Center for Ecogenetics and Environmental Health NIEHS grant 5P30ESO7033-03, Center of Human Development and Disability, The Environmental Pathology Training grant (T32ES07032), and the Seattle Chapter of the ARCS Foundation.

### References

- [1] B. Anlar, P. Atilla, N. Cakar, M. Tombakoglu, A. Bulun, Apoptosis in the developing human brain: a preliminary study of the frontal region, *Early Human Development* 71 (2003) 53–60.
- [2] B.A. Barres, I.K. Hart, H.S.R. Coles, J.F. Burne, J.T. Voyvodic, M.C. Raff, Cell-death and control of cell-survival in the oligodendrocyte lineage, *Cell* 70 (1992) 31–46.
- [3] A.J. Blaschke, K. Staley, J. Chun, Widespread programmed cell death in proliferative and postmitotic regions of the fetal cerebral cortex, *Development* 122 (1996) 1165–1174.
- [4] A.J. Blaschke, J.A. Weiner, J. Chun, Programmed cell death is a universal feature of embryonic and postnatal neuroproliferative regions throughout the central nervous system, *Journal of Comparative Neurology* 396 (1998) 39–50.
- [5] L. Bondolfi, M. Calhoun, F. Ermini, H.G. Kuhn, K.H. Wiederhold, L. Walker, M. Staufenbiel, M. Jucker, Amyloid-associated neuron loss and gliogenesis in the neocortex of amyloid precursor protein transgenic mice, *Journal of Neuroscience* 22 (2002) 515–522.
- [6] L. Cai, N.L. Hayes, R.S. Nowakowski, Local homogeneity of cell cycle length in developing mouse cortex, *Journal of Neuroscience* 17 (1997) 2079–2087.
- [7] L. Cai, N.L. Hayes, T. Takahashi, V.S. Caviness, R.S. Nowakowski, Size distribution of retrovirally marked lineages matches prediction from population measurements of cell cycle behavior, *Journal of Neuroscience Research* 69 (2002) 731–744.
- [8] M.E. Calhoun, K.H. Wiederhold, D. Abramowski, A.L. Phinney, A. Probst, C. Sturchler-Pierrat, M. Staufenbiel, B. Sommer, M. Jucker, Neuron loss in APP transgenic mice, *Nature* 395 (1998) 755–756.
- [9] V.S. Caviness, T. Goto, T. Tarui, T. Takahashi, P.G. Bhide, R.S. Nowakowski, Cell output, cell cycle duration and neuronal specification: a

- model of integrated mechanisms of the neocortical proliferative process, *Cerebral Cortex* 13 (2003) 592–598.
- [10] M. Chiourel, Mathematical biology—life is a game of numbers, *Nature* 408 (2000) 900–901.
- [11] J. Chun, Cell death, DNA breaks and possible rearrangements: an alternative view, *Trends in Neurosciences* 23 (2000) 407–408.
- [12] W.M. Cowan, J.W. Fawcett, D.D. O’Leary, B.B. Stanfield, Regressive events in neurogenesis, *Science* 225 (1984) 1258–1265.
- [13] M.E. Csete, J.C. Doyle, Reverse engineering of biological complexity, *Science* 295 (2002) 1664–1669.
- [14] E.H. Davidson, J.P. Rast, P. Oliveri, A. Ransick, C. Caletani, C.H. Yuh, T. Minokawa, G. Amore, V. Hinman, C. Arenas-Mena, O. Otim, C.T. Brown, C.B. Livi, P.Y. Lee, R. Revilla, A.G. Rust, Z.J. Pan, M.J. Schilstra, P.J.C. Clarke, M.I. Arnone, L. Rowen, R.A. Cameron, D.R. McClay, L. Hood, H. Bolouri, A genomic regulatory network for development, *Science* 295 (2002) 1669–1678.
- [15] E.J. de la Rosa, F. de Pablo, Cell death in early neural development: beyond the neurotrophic theory, *Trends in Neurosciences* 23 (2000) 454–458.
- [16] P. Dearden, M. Akam, Segmentation in silico, *Nature* 406 (2000) 131–132.
- [17] T.L. Deckwerth, E.M. Johnson, Temporal Analysis of Events Associated with Programmed Cell-Death (Apoptosis) of Sympathetic Neurons Deprived of Nerve Growth-Factor, *Journal of Cell Biology* 123 (1993) 1207–1222.
- [18] M. Deshmukh, E.M. Johnson, Programmed cell death in neurons: focus on the pathway of nerve growth factor deprivation-induced death of sympathetic neurons, *Molecular Pharmacology* 51 (1997) 897–906.
- [19] K. Dikranian, M.J. Ishimaru, T. Tenkova, J. Labryere, Y.Q. Qin, C. Ikonomidou, J.W. Olney, Apoptosis in the in vivo mammalian forebrain, *Neurobiology of Disease* 8 (2001) 359–379.
- [20] C. D’Sa-Eipper, J.R. Leonard, G. Putcha, T.S. Zheng, R.A. Flavell, P. Rakic, K. Kuida, K.A. Roth, DNA damage-induced neural precursor cell apoptosis requires p53 and caspase 9 but neither Bax nor caspase 3, *Development* 128 (2001) 137–146.
- [21] S.J. Duffell, A.R. Soames, S. Gunby, Morphometric analysis of the developing rat brain, *Toxicologic Pathology* 28 (2000) 157–163.
- [22] R.E. Ellis, J.Y. Yuan, H.R. Horvitz, Mechanisms and Functions of Cell-Death, *Annual Review of Cell Biology* 7 (1991) 663–698.
- [23] E.M. Faustman, T. Lewandowski, R. Ponce, S. Bartell, Biologically based dose–response models for developmental toxicants: lessons from methylmercury, *Inhalation Toxicology* 11 (1999) 559–572.
- [24] I. Ferrer, M. Hernandezmarti, E. Bernet, E. Galofre, Formation and growth of the cerebral convolutions: 1. Postnatal-development of the median-suprasylvian gyrus and adjoining sulci in the cat, *Journal of Anatomy* 160 (1988) 89–100.
- [25] I. Ferrer, E. Bernet, E. Soriano, T. del Rio, M. Fonseca, Naturally occurring cell death in the cerebral cortex of the rat and removal of dead cells by transitory phagocytes, *Neuroscience* 39 (1990) 451–458.
- [26] I. Ferrer, E. Soriano, J. Del Rio, S. Alcantara, C. Auladell, Cell death and removal in the cerebral cortex during development, *Progress in Neurobiology* 39 (1992) 1–43.
- [27] E.C. Gilmore, K. Herrup, R.S. Nowakowski, V.S. Caviness, Cell death, DNA breaks and possible rearrangements: an alternative view—Reply, *Trends in Neurosciences* 23 (2000) 408–409.
- [28] E.C. Gilmore, R.S. Nowakowski, V.S. Caviness, K. Herrup, Cell birth, cell death, cell diversity and DNA breaks: how do they all fit together? *Trends in Neurosciences* 23 (2000) 100–105.
- [29] J. Gohlke, W. Griffith, S. Bartell, T. Lewandowski, E. Faustman, A computational model for neocortical neurogenesis predicts ethanol-induced neocortical neuron number deficits, *Developmental Neuroscience* 24 (2002) 467–477.
- [30] C. Guerri, Neuroanatomical and neurophysiological mechanisms involved in central nervous system dysfunctions induced by prenatal alcohol exposure, *Alcoholism, Clinical and Experimental Research* 22 (1998) 304–312.
- [31] A.R. Harvey, D. Robertson, Time-course and extent of retinal ganglion-cell death following ablation of the superior colliculus in neonatal rats, *Journal of Comparative Neurology* 325 (1992) 83–94.
- [32] H. Haug, Brain sizes, surfaces, and neuronal sizes of the cortex cerebri: a stereological investigation of man and his variability and a comparison with some mammals (primates, whales, marsupials, insectivores, and one elephant), *American Journal of Anatomy* 180 (1987) 126–142.
- [33] T.F. Haydar, C.Y. Kuan, R.A. Flavell, P. Rakic, The role of cell death in regulating the size and shape of the mammalian forebrain, *Cerebral Cortex* 9 (1999) 621–626.
- [34] T.F. Haydar, R. Nowakowski, P. Yarowsky, B. Krueger, Role of founder cell deficit and delayed neurogenesis in microencephaly of the Trisomy 16 mouse, *Journal of Neuroscience* 20 (2000) 4156–4164.
- [35] G.M. Horsburgh, A.J. Sefton, Cellular degeneration and synaptogenesis in the developing retina of the rat, *Journal of Comparative Neurology* 263 (1987) 553–566.
- [36] K. Hoshino, Y. Kameyama, Developmental-Stage-Dependent Radio-sensitivity of Neural Cells in the Ventricular Zone of Telencephalon in Mouse and Rat Fetuses, *Teratology* 37 (1988) 257–262.
- [37] K. Hoshino, Y. Kameyama, M. Inouye, Split-Dose effect of X-Irradiation on the induction of cell death in the fetal mouse brain, *Journal of Radiation Research* 32 (1991) 23–27.
- [38] R.J. Kavlock, Recent advances in mathematical modeling of developmental abnormalities using mechanistic information, *Reproductive Toxicology* 11 (1997) 423–434.
- [39] H. Kitano, Computational systems biology, *Nature* 420 (2002) 206–210.
- [40] C.Y. Kuan, K.A. Roth, R.A. Flavell, P. Rakic, Mechanisms of programmed cell death in the developing brain, *Trends in Neurosciences* 23 (2000) 291–297.
- [41] K. Kuida, T.S. Zheng, S.Q. Na, C.Y. Kuan, D. Yang, H. Karasuyama, P. Rakic, R.A. Flavell, Decreased apoptosis in the brain and premature lethality in CPP32-deficient mice, *Nature* 384 (1996) 368–372.
- [42] K. Kuida, T.F. Haydar, C.Y. Kuan, Y. Gu, C. Taya, H. Karasuyama, M.S.S. Su, P. Rakic, R.A. Flavell, Reduced apoptosis and cytochrome *c*-mediated caspase activation in mice lacking Caspase 9, *Cell* 94 (1998) 325–337.
- [43] J.R. Leonard, B.J. Klocke, C. D’Sa, R.A. Flavell, K.A. Roth, Strain-dependent neurodevelopmental abnormalities in caspase-3-deficient mice, *Journal of Neuropathology and Experimental Neurology* 61 (2002) 673–677.
- [44] B. Leroux, W. Leisenring, S. Moolgavkar, E.M. Faustman, A Biologically-Based Dose–Response Model for developmental toxicology, *Risk Analysis* 16 (1996) 449–458.
- [45] L. Lossi, A. Merighi, In vivo cellular and molecular mechanisms of neuronal apoptosis in the mammalian CNS, *Progress in Neurobiology* 69 (2003) 287–312.
- [46] M. Mesulam, From sensation to cognition, *Brain* 121 (1998) 1013–1052.
- [47] M.W. Miller, R. Nowakowski, Effect of prenatal exposure to ethanol on the cell cycle kinetics and growth fraction in the proliferative zones of fetal rat cerebral cortex, *Alcoholism, Clinical and Experimental Research* 15 (1991) 229–232.
- [48] M.W. Miller, P.E. Kuhn, Cell cycle kinetics in fetal rat cerebral cortex: effects of prenatal treatment with ethanol assessed by a cumulative labeling technique with flow cytometry, *Alcoholism, Clinical and Experimental Research* 19 (1995) 233–237.
- [49] S. Miyama, T. Takahashi, R. Nowakowski, V. Caviness, A gradient in the duration of the G1 phase in the murine neocortical proliferative epithelium, *Cerebral Cortex* 7 (1997) 678–689.
- [50] A. Moller, P. Strange, H. Gundersen, Efficient estimation of cell volume and number using the nucleator and the disector, *Journal of Microscopy* 159 (1990) 61–71.
- [51] S.M. Mooney, R.M.A. Napper, J.R. West, Long-term effect of post-natal alcohol exposure on the number of cells in the neocortex of the

- rat: a stereological study, *Alcoholism, Clinical and Experimental Research* 20 (1996) 615–623.
- [52] G. Neves, J. Zucker, M. Daly, A. Chess, Stochastic yet biased expression of multiple Dscam splice variants by individual cells, *Nature Genetics* (2004) 240–246.
- [53] D. Nijhawan, N. Honarpour, X. Wang, Apoptosis in neuronal development and disease, *Annual Review of Neuroscience* 23 (2000) 73–87.
- [54] S.C. Noctor, V. Martinez-Cerdenio, L. Ivic, A.R. Kriegstein, Cortical neurons arise in symmetric and asymmetric division zones and migrate through specific phases, *Nature Neuroscience* 7 (2004) 136–144.
- [55] R.S. Nowakowski, V.S. Caviness, N.L. Hayes, Population dynamics during cell proliferation and neurogenesis in the developing murine neocortex, *Results and Problems in Cell Differentiation* 39 (2002) 1–25.
- [56] R. Oppenheim, Cell death during development of the nervous system, *Annual Review of Neuroscience* 14 (1991) 453–501.
- [57] Y. Otsuki, Z. Li, M.-A. Shibata, Apoptotic detection methods—from morphology to gene, *Progress in Histochemistry and Cytochemistry* 38 (2003) 275–335.
- [58] M. Pompeiano, A.J. Blaschke, R.A. Flavell, A. Srinivasan, J. Chun, Decreased apoptosis in proliferative and postmitotic regions of the caspase 3-deficient embryonic central nervous system, *Journal of Comparative Neurology* 423 (2000) 1–12.
- [59] M.C. Raff, B.A. Barres, J.F. Burne, H.S. Coles, Y. Ishizaki, M.D. Jacobson, Programmed Cell-Death and the Control of Cell-Survival—Lessons from the Nervous-System, *Science* 262 (1993) 695–700.
- [60] S. Rakic, N. Zecevic, Programmed cell death in the developing human telencephalon, *European Journal of Neuroscience* 12 (2000) 2721–2734.
- [61] S.K. Rehen, M.J. McConnell, D. Kaushal, M.A. Kingsbury, A.H. Yang, J. Chun, Chromosomal variation in neurons of the developing and adult mammalian nervous system, *Proceedings of the National Academy of Sciences of the United States of America* 98 (2001) 13361–13366.
- [62] K. Reznikov, D. van der Kooy, Variability and partial synchrony of the cell cycle in the germinal zone of the early embryonic cerebral cortex, *Journal of Comparative Neurology* 360 (1995) 536–554.
- [63] A. Rockel, R. Horns, T. Powell, The basic uniformity of structure of the neocortex, *Brain* 103 (1980) 221–244.
- [64] J.M. Sekiguchi, Y. Gao, Y. Gu, K. Frank, Y. Sun, J. Chaudhuri, C. Zhu, H.L. Cheng, J. Manis, D. Ferguson, L. Davidson, M.E. Greenberg, F.W. Alt, Nonhomologous end-joining proteins are required for V(D)J recombination, normal growth, and neurogenesis, *Cold Spring Harbor Symposia on Quantitative Biology* 64 (1999) 169–181.
- [65] A. Shuz, G. Palm, Density of neurons and synapses in the cerebral cortex of the mouse, *Journal of Comparative Neurology* 286 (1989) 442–455.
- [66] R. Spreafico, C. Frassoni, P. Arcelli, M. Selvaggio, S. De Biasi, In situ labeling of apoptotic cell death in the cerebral cortex and thalamus of rats during development, *Journal of Comparative Neurology* 363 (1995) 281–295.
- [67] W.B. Stewart, L.R. Ment, M. Schwartz, Chronic postnatal hypoxia increases the numbers of cortical neurons, *Brain Research* 760 (1997) 17–21.
- [68] P. Strange, A. Moller, O. Ladefoged, H.R. Lam, J.J. Larsen, P. Arliensborg, Total Number and Mean Cell-Volume of Neocortical Neurons in Rats Exposed to 2,5-Hexanedione with and without Acetone, *Neurotoxicology and Teratology* 13 (1991) 401–406.
- [69] T. Takahashi, R. Nowakowski, V. Caviness, Cell cycle parameters and patterns of nuclear movement in the neocortical proliferative zone of the fetal mouse, *Journal of Neuroscience* 13 (1993) 820–833.
- [70] T. Takahashi, R. Nowakowski, V. Caviness, The cell cycle of the pseudostratified ventricular epithelium of the embryonic murine cerebral wall, *Journal of Neuroscience* 15 (1995) 6046–6057.
- [71] T. Takahashi, R. Nowakowski, V. Caviness, Early ontogeny of the secondary proliferative population of the embryonic murine cerebral wall, *Journal of Neuroscience* 15 (1995) 6058–6068.
- [72] T. Takahashi, R. Nowakowski, V. Caviness, The leaving or Q fraction of the murine cerebral proliferative epithelium: a general model of neocortical neurogenesis, *Journal of Neuroscience* 16 (1996) 6183–6196.
- [73] T. Takahashi, R. Nowakowski, V. Caviness, The mathematics of neocortical neurogenesis, *Developmental Neuroscience* 19 (1997) 17–22.
- [74] D. Thieffry, L. Sanchez, Dynamical modelling of pattern formation during embryonic development, *Current Opinion in Genetics & Development* 13 (2003) 326–330.
- [75] D. Thomaidou, M.C. Mione, J.F. Cavanagh, J.G. Parnavelas, Apoptosis and its relation to the cell cycle in the developing cerebral cortex, *Journal of Neuroscience* 17 (1997) 1075–1085.
- [76] C. Verney, T. Takahashi, P. Bhide, R. Nowakowski, V. Caviness, Independent controls for neocortical neuron production and histogenetic cell death, *Developmental Neuroscience* 22 (2000) 125–138.
- [77] G. von Dassow, E. Meir, E.M. Munro, G.M. Odell, The segment polarity network is a robust development module, *Nature* 406 (2000) 188–192.
- [78] J.T. Voyvodic, J.F. Burne, M.C. Raff, Quantification of normal cell death in the rat retina: implications for clone composition in cell lineage analysis, *European Journal of Neuroscience* 7 (1995) 2469–2478.
- [79] D. Heumann, G. Leuba, Neuronal death in the development and aging of the cerebral cortex of the mouse, *Neuropathology and Applied Neurobiology* 9 (1983) 297–311.
- [80] M.W. Miller, Relationship of the time of origin and death of neurons in rat somatosensory cortex: barrel versus septal cortex and projection versus local circuit neurons, *Journal of Comparative Neurology* 355 (1995) 6–14.
- [81] J.L. Nunez, D.M. Lauschke, J.M. Juraska, Cell death in the development of the posterior cortex in male and female rats, *Journal of Comparative Neurology* 436 (2001) 32–41.